# A Comparative Statistical Study of Some Proposed Six-Port Junction Designs

MARK BERMAN, PETER I. SOMLO, FELLOW, IEEE, AND MICHAEL J. BUCKLEY

*Abstract* —Reflection coefficient measurements obtained from six-port reflectometers are analyzed from a statistical and geometrical point of view. The analysis concentrates on the effect of using noisy power meters, and a simply computed, geometrically interpretable estimator of the reflection coefficient possessing certain optimality properties is derived. A suitable performance measure for this estimator is calculated for a number of different six-port designs as the true reflection coefficient ranges over the area of the Smith chart. For each design, a contour map of the measure allows for easy comparison of the designs in different regions of the Smith chart.

## I. Introduction

SINCE THE FIRST proposals of Engen and Hoer [1] and Hoer [2] to measure impedance (besides power, voltage, and current) using six-port junctions equipped with a number of power meters, a number of proposals have been made on how to construct six-port junctions for optimum performance. The reported optimizations confined their aims to either minimizing the frequency sensitivity [3] or permitting the interpretations of swept visual displays [4]. In this paper, the optimality criterion used is statistically based, and is derived via a model of measurement noise. Although there exist papers which use statistical ideas to construct estimators of the reflection coefficient [5], [6], this paper is the first (as far as we know) to use such ideas to compare six-port junction *designs*. A by-product of the statistical analysis is the construction of a simply computed, geometrically interpretable estimator of the reflection coefficient possessing certain optimality properties not shared by other estimators.

What prompted this investigation was the fact that in the CSIRO National Measurement Laboratory, a conscious choice was made to build and use six-ports with power meters located at ports in phase quadrature (in conjunction with a power meter responding to incident power) [7]–[9]. The reason for this choice was the accumulated experience gained with the locating reflectometer [10], which provided, besides the real-time time-domain display, a real-time analog Smith chart display. This useful facility is provided simply by differencing pairs of power meters phased 180° apart. Intuitively, it was felt that a circuit which provides a good real-time analog Smith chart display should not perform poorly when full six-port theory is applied to enhance its accuracy.

Manuscript received September 8, 1986; revised June 16, 1987.

M. Berman and M. J. Buckley are with the Commonwealth Scientific and Industrial Research Organisation, Division of Mathematics and Statistics, National Measurement Laboratory, Lindfield, N.S.W. 2070, Australia.

P. I. Somlo is with the Commonwealth Scientific and Industrial Research Organisation, Division of Applied Physics, National Measurement Laboratory, Lindfield, N.S.W. 2070, Australia.

IEEE Log Number 8716599.

## II. Mathematical Background and Geometrical Interpretation

The fundamental six-port equations were given by Engen [11] and later shown to be derivable in a simple manner by Hunter and Somlo [12] as

$$\frac{P_i}{P_0} = s_i \left| \frac{\Gamma - B_i}{\Gamma - B_0} \right|^2, \qquad i = 1,2,3 \tag{1}$$

where $\Gamma$ is the unknown reflection coefficient, $P_i$ are the power meter readings, $s_i$ are known real constants, and $B_i$ are known complex constants. Three power meter readings are normalized to the fourth; therefore only *power ratios* need to be observed (thus negating the need to use calibrated power meters). Engen [11] has shown that equations (1) represent circles in the complex plane as $P_i/P_0$ is held constant, and therefore any measurement of $\Gamma$ may be interpreted as finding the *common* intersection point of three circles which simultaneously satisfy three equations for the measured power ratios. (The calibration of the six-port is the inverse operation: finding the centers of circles from known values of $\Gamma$. This problem will not be dealt with here.) Even when a reflectometer is already calibrated, the three circles do not intersect at a common point, principally because of noise in the power meter readings.

Each of the three *pairs* of circles will usually produce two intersection points. Typically, three of the six intersection points (one from each pair of circles) will form a cluster. Each of these three points is an estimator of $\Gamma$. The first aim of our paper is to show how, for any given six-port design, one should combine the three estimators to produce the (approximately) optimal estimator of $\Gamma$.

A number of six-port junction designs have been proposed in the literature. These differ from one another in the placement of the centers of the three "Engen circles" on the complex reflection coefficient plane (extended Smith chart). The second (and main) aim of the present paper is to make an objective comparison, using statistical techniques, of some of the six-port junction design suggestions, namely those of Engen [11], Engen and Hoer [13], Groll and Kohl [14], Somlo and Hunter [7], and Griffin *et al.*

0018-9480/87/1100-0971$01.00 

[15]. This is not a comprehensive list of all six-port proposals to date, but hopefully is sufficient to aid future users to make a choice.

Of course, it is possible to have $n$-port designs with $n > 6$. This will produce more than three circles, and more than three estimators of their common intersection point. Although the theory to be presented in this paper could in principle be extended to such designs, they will not be considered in this paper.

## III. Statistical Review and a New Model

Engen [5] has suggested using the maximum likelihood estimator of $\Gamma$, assuming that the $P_i$'s are independent Gaussian random variables, each with a (possibly) different but known variance. This may not be robust against departures from Gaussianity and requires a nonlinear minimization, which would be difficult to apply in real time. Herscher and Carroll [6] propose linear combinations of the individual estimators of $\Gamma$. Specifically, the unbiased linear combination of the real parts of the estimators with smallest variance is derived; an entirely analogous situation holds for the imaginary parts. Although this procedure is computationally simple and is independent of the distributional properties of the noise, it has some other drawbacks. First, because the real and imaginary parts are considered separately, their final estimator of $\Gamma$ is not in general invariant under rotations of the axes; nor will the variances of the components of the estimator be as small as they could be if the real and imaginary parts are considered jointly. Second, in their calculations, Herscher and Carroll assume that the power ratios are uncorrelated. Since the power ratios have a common power meter reading in the denominator (see (1)), such an assumption may not be justified. In addition, the generality of the solution in [6], in terms of general calibration constants and differing power meter reading variances, does not easily lend itself to a comparison of six-port designs.

The approach adopted here overcomes to a great extent the objections detailed above. This is partly achieved by making simplifying assumptions which lead to a model with few parameters. Such a model is easier to handle and at the same time often gives a reasonable approximation to reality.

Formulas for the centers and radii of the circles defined by (1) are derived, for instance, in [16]. However, it will for the most part be more convenient to use different notation for the remainder of the paper. In particular, our analysis will be performed in the real Cartesian plane rather than in the complex plane. Let $C_i = (\xi_i, \eta_i)$ and $R_i$, $i = 1,2,3$, denote the centers and radii of the three *true* circles (i.e., if there were no measurement noise present), and let $\Gamma = (\mu, \nu)$ denote the common intersection point of the three circles.

If it is assumed that a six-port has been *calibrated already* and is now used for *measurement*, then [16] for practical purposes the approximation can be used that the centers of the circles are known and fixed. (The more the reference power meter responds primarily to incident power, the more this will be so.) If a measurement is performed, then system noise will affect the observed power ratios only; hence the radii of the circles will have a superimposed noise component. Let $\hat{R}_i$ denote the estimator of $R_i$. Then we can write

$$\hat{R}_i = R_i + \epsilon_i, \qquad i = 1,2,3 \tag{2}$$

where $\epsilon_i$ is the measurement error in $\hat{R}_i$. In most practical situations, the three radii are of similar size, so that one might expect their variances to be similar. We shall therefore assume that the errors have zero mean and *common* variance $\sigma^2$. Also, as noted above, even if the power meter readings are uncorrelated, the normalizing reading $P_0$ in (1) will induce correlation between the power ratios and hence in the errors. For simplicity, let $P_i = 1,2,3$ have a common signal-to-noise ratio, $SN_1$, and let $P_0$ have a (possibly different) signal-to-noise ratio, $SN_0$. It can be shown using Taylor series expansions that, provided $SN_0$ and $SN_1$ are reasonably large, the correlation of $\epsilon_i$ and $\epsilon_j$ for $j \neq i$ is a nonnegative number, say $\rho$, where $\rho \doteq 0.5$ if $SN_1/SN_0 = 1$, $\rho \to 0$ if $SN_1/SN_0 \to \infty$, and $\rho \to 1$ if $SN_1/SN_0 \to 0$. Details will not be presented here. We shall henceforth assume a *common* nonnegative correlation $\rho$ among the errors. Note that this model depends only on errors in the $R_i$'s and so is completely independent of the real and imaginary axes; one would expect, therefore, an estimation procedure which is invariant under rotation of the axes.

It will be convenient to let $\hat{\Gamma}_i = (\hat{\mu}_i, \hat{\nu}_i)$, $i = 1,2,3$, denote the estimator of $\Gamma$ obtained from circles $i-1$ and $i+1$, where $\hat{\Gamma}_i \equiv \hat{\Gamma}_{i-3}$. When the two circles have two intersection points (which for a six-port will usually be true), it is easily shown that

$$\begin{bmatrix} \hat{\mu}_i \\ \hat{\nu}_i \end{bmatrix} = \begin{bmatrix} \xi_{i-1} \\ \eta_{i-1} \end{bmatrix} + \frac{a_i}{d_i}\begin{bmatrix} \xi_{i+1} - \xi_{i-1} \\ \eta_{i+1} - \eta_{i-1} \end{bmatrix} \pm \frac{b_i}{d_i}\begin{bmatrix} \eta_{i+1} - \eta_{i-1} \\ \xi_{i-1} - \xi_{i+1} \end{bmatrix}, \qquad i = 1,2,3 \tag{3}$$

where

$$a_i = \left(\hat{R}_{i-1}^2 - \hat{R}_{i+1}^2 + d_i^2\right)/2d_i, \quad b_i = \left(\hat{R}_{i-1}^2 - a_i^2\right)^{\frac{1}{2}}$$

$$d_i = \left\{\left(\xi_{i+1} - \xi_{i-1}\right)^2 + \left(\eta_{i+1} - \eta_{i-1}\right)^2\right\}^{\frac{1}{2}} \tag{4}$$

and $(\xi_i, \eta_i, \hat{R}_i) \equiv (\xi_{i-3}, \eta_{i-3}, \hat{R}_{i-3})$ for all $i$.

## IV. The Approximately Optimal Linear Estimator of $\Gamma$

As in [6], we shall consider linear combinations of the three estimators $\hat{\Gamma}_i$, $i = 1,2,3$, and shall seek those linear combinations of $(\hat{\mu}_i, \hat{\nu}_i)$, $i = 1,2,3$, which are minimum variance linear unbiased estimators (MVLUE's) for both $\mu$ and $\nu$. Such estimators are computationally simple, independent of the distributional properties of the noise, and invariant under rotations of the axes. In order to find such estimators, one needs to know the variances and covariances of $(\hat{\mu}_i, \hat{\nu}_i)$, $i = 1,2,3$. Unfortunately, because $(\hat{\mu}_i, \hat{\nu}_i)$ is a nonlinear function of $\hat{R}_{i-1}$ and $\hat{R}_{i+1}$, it is not possible to obtain exact formulas for these. However, if $\sigma$ is small

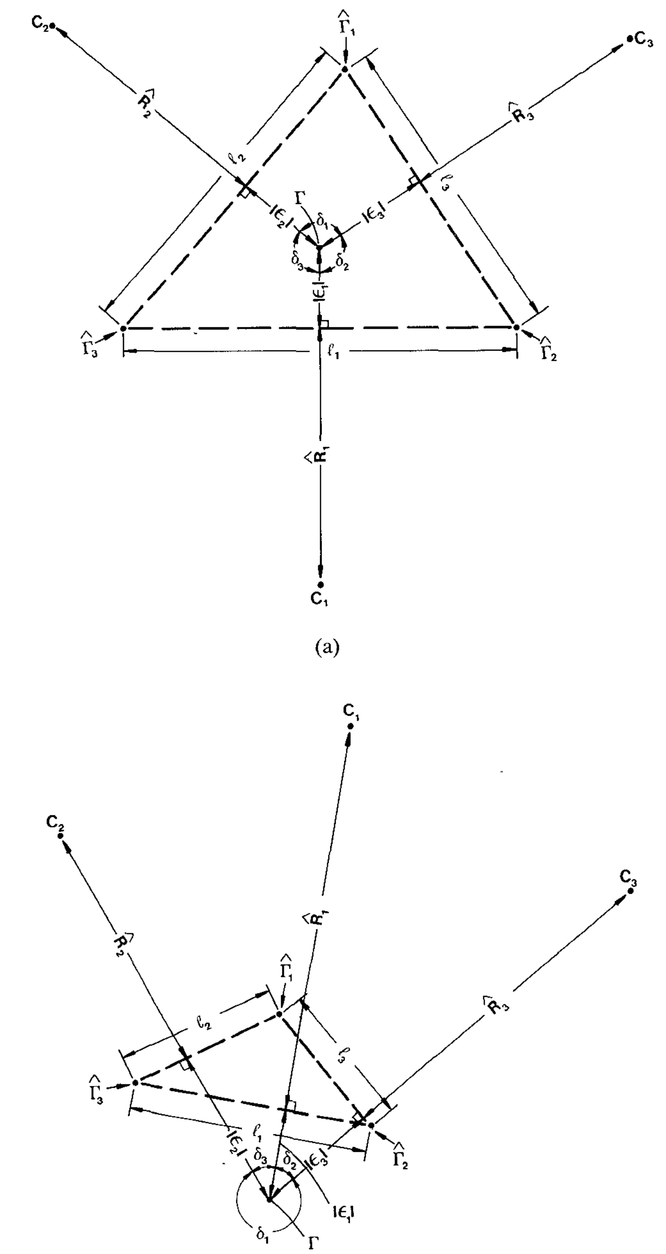

Fig. 1. (a) Approximate representation of errors in measurement of radii when $0 < \delta_i < \pi$, $i = 1,2,3$. Broken lines represent circumferences of observed circles. (b) Approximate representation of errors in measurement of radii when $\delta_1 > \pi$, $0 < \delta_2$, $\delta_3 < \pi$. Broken lines represent circumferences of observed circles. (a) (b)

relative to the $R_i$'s, we can insert (2) into (3) and (4) and perform a Taylor series expansion of (3) in terms of $\epsilon_{i-1}$ and $\epsilon_{i+1}$ to first order to obtain a reasonable approximation to these quantities. It can be shown that this is equivalent to assuming that the circumferences of the circles are linear in the neighborhood of their intersection points. This linear approximation to the problem is illustrated geometrically in Fig. 1(a) and (b). In either of these, we see that the three lines forming the triangle with vertices $\hat{\Gamma}_i$, $i = 1,2,3$, are each perpendicular to one of the lines joining $\Gamma$ to the circle centers $C_i$, $i = 1,2,3$. Let $\theta_i$ denote the angle between the *directed* line $\Gamma, C_i$ and the positive $x$ axis, and let $\alpha_i$ denote the $y$-axis intercept of the line joining $\hat{\Gamma}_{i-1}$ and $\hat{\Gamma}_{i+1}$. Then it is straightforward to show that

$$\epsilon_i = \nu \sin\theta_i + \mu \cos\theta_i - \alpha_i \sin\theta_i, \qquad i = 1,2,3. \tag{5}$$

Note that (at least for the linearized version of our model) $\alpha_i$ and $\theta_i$ are observed (the latter because $\theta_i - \pi/2$ is the angle joining $\hat{\Gamma}_{i-1}$ and $\hat{\Gamma}_{i+1}$). The importance of (5) is that $\epsilon_i$ can be expressed as a linear function of the unknown parameters $\mu$ and $\nu$, and so this is a special case of the general linear model [17], whose statistical properties are well known. In particular, there is a standard formula for the MVLUE's of $\mu$ and $\nu$. However, this will not be in terms of the $\hat{\Gamma}_i$'s. Additional algebra, however, leads to the MVLUE formula

$$\hat{\Gamma} = \sum_{i=1}^{3} \omega_i \hat{\Gamma}_i \tag{6}$$

where

$$\omega_i = m_i\{m_i + \rho(m_{i-1} + m_{i+1})\}/D, \qquad i = 1,2,3 \tag{7}$$

$$D = (1-\rho)\sum_{i=1}^{3} m_i^2 + \rho\left(\sum_{i=1}^{3} m_i\right)^2 \tag{8}$$

$$m_i = l_i \qquad \text{if } \delta_i \leqslant \pi$$
$$= -l_i \qquad \text{if } \delta_i > \pi, \qquad i = 1,2,3 \tag{9}$$

where $l_i$ is the length of the side of the triangle opposite $\hat{\Gamma}_i$, and $\delta_i$ is the nonnegative angle subtended at $\Gamma$ by $C_{i-1}$ and $C_{i+1}$, with $m_i \equiv m_{i-3}$, $\delta_i \equiv \delta_{i-3}$, and $C_i \equiv C_{i-3}$ (see Fig. 1(a) and (b)). Details of the derivation of (6) will not be given here but will be supplied on request. Note that

$$\sum_{i=1}^{3} \omega_i = 1 \tag{10}$$

$$\sum_{i=1}^{3} \delta_i = 2\pi. \tag{11}$$

Regarding (9), in most practical situations it will be easy to see whether any of the $\delta_i$'s is greater than $\pi$. When this is not the case (as in Fig. 1(a)), all the $m_i$'s will be positive, and so will all the $\omega_i$'s. Now any point $\hat{\Gamma}$ in the plane can be written as the sum of any three other points in the plane in the form (6) where the $\omega_i$'s satisfy (10). If all the $\omega_i$'s are positive, then $\hat{\Gamma}$ lies inside the triangle formed by $\hat{\Gamma}_i$, $i = 1,2,3$; this will always be the case if all the $\delta_i$'s $\leqslant \pi$. However, this is not necessarily so if one of the $\delta_i$'s is greater than $\pi$ (see Fig. 1(b)). For this case, it is informative to consider the two extremes $\rho = 0$ and $\rho = 1$. When $\rho = 0$, we see from (7) that $\omega_i \propto m_i^2 = l_i^2$ so that it is always positive, and hence $\hat{\Gamma}$ lies inside the triangle. On the other hand, when $\rho = 1$ and say, $\delta_1 > \pi$, it can be shown that $\omega_1 < 0$, while $\omega_2 > 0$, $\omega_3 > 0$, so that $\hat{\Gamma}$ lies outside the triangle. Why should this be so? When $\rho = 1$, all the $\epsilon_i$'s must have the same sign. When $\delta_1 > \pi$, it is easily seen that no point inside the triangle can satisfy this requirement (see Fig. 1(b) for the case where all the $\epsilon_i$'s are negative). When $0 < \rho < 1$ and $\delta_1 > \pi$, $\hat{\Gamma}$ lies inside the triangle if and only if $\omega_1 > 0$; i.e., $m_1 < -\rho(m_2 + m_3)$ or, equivalently, $\sin\delta_1 < -\rho(\sin\delta_2 + \sin\delta_3)$ because $m_i \propto \sin\delta_i$.

The above theory is based on a model which approximates the circumferences of the circles by straight lines in the neighborhood of their intersection point. To investigate the validity of this approximation, we carried out some simulations for various angular configurations of circle centers about $\Gamma$, with $\rho = 0$ and 0.5, the $R_i$'s all equal, and $\sigma/R_i = 0.01$ and 0.1, respectively. As our measure of the adequacy of the linear approximation, we used the simple *rotationally invariant* mean squared distance (MSD) of $(\hat{\mu}, \hat{\nu})$ from $(\mu, \nu)$. For each angular configuration and value of $\sigma/R_i$, we estimated the MSD by averaging the square of the distance from $(\hat{\mu}, \hat{\nu})$ to $(\mu, \nu)$ obtained in each of 10 000 simulations. This can be compared with the following *theoretical* value of MSD derived using general linear model theory:

$$\mathrm{MSD} = E\left\{(\hat{\mu}-\mu)^2 + (\hat{\nu}-\nu)^2\right\} \doteq \mathrm{Var}(\hat{\mu}) + \mathrm{Var}(\hat{\nu})$$
$$\doteq \sigma^2(1-\rho)\left\{3(1+\rho) - 2\rho\sum_{i=1}^{3}\cos\delta_i\right\}$$
$$\Bigg/\left\{(1-\rho)\sum_{i=1}^{3}\sin^2\delta_i + \rho\left(\sum_{i=1}^{3}\sin\delta_i\right)^2\right\}. \tag{12}$$

Full details of the simulations will not be given here. However, the main points to emerge are that when $\sigma/R_i = 0.01$, the simulated MSD's are within about 5 percent of the theoretical MSD's except when $\rho = 0.5$ and one of the $\delta_i$'s equals $\pi$; in this last case, the simulated MSD is about 15 percent larger than the theoretical approximation. When $\rho = 0$ and $\sigma/R_i = 0.1$, similar results are obtained, although when one of the $\delta_i$'s is near 0 or $\pi$, the simulated MSD is again about 15 percent larger than the theoretical approximation. When $\rho = 0.5$ and $\sigma/R_i = 0.1$, simulations were not possible because there is a small but significant probability that none of the three circles intersect!

The case when one of the $\delta_i$'s is at 0 or $\pi$ deserves special comment. When this is so, the *true* circles will touch tangentially; the *observed* circles may therefore not touch at all, leaving only two intersection points for estimation instead of three. However, the above theory still leads to a sensible result. In particular, the triangles in Fig. 1(a) and (b) become two parallel lines intersecting a third line. The estimator (6) is then just the average of the two intersection points, and this is therefore the recommended estimator of $\Gamma$ when only two intersection points are available.

## V. Practical Implementation

Numerous authors have used (1) to show that $\Gamma$ can be expressed as

$$\Gamma = \left(\sum_{i=0}^{3} F_i P_i + j\sum_{i=0}^{3} G_i P_i\right)\Bigg/\sum_{i=0}^{3} H_i P_i \tag{13}$$

where $F_i$, $G_i$, and $H_i$, $i = 0,1,2,3$, are real constants. When the six-port is calibrated, these constants can be computed and then used at subsequent measurements to obtain $\Gamma$ very rapidly. However, it is not clear whether, in the presence of noise, (13) is using the available information in an optimal way.

In view of the statistical theory of Section IV, we have found it preferable to use (6), at the expense of a few extra seconds of computing time, and in addition to obtain an estimate of $\sigma$. From general linear model theory [17] and additional algebra, an unbiased estimator of $\sigma^2$ is

$$\hat{\sigma}^2 = 4\Delta^2/D \tag{14}$$

where $D$ is given by (8) and

$$\Delta = \frac{1}{2}\left|\sum_{i=1}^{3}(\hat{\mu}_i\hat{\nu}_{i-1} - \hat{\mu}_{i-1}\hat{\nu}_i)\right|$$
$$= \frac{1}{4}\left\{\left(\sum_{i=1}^{3} l_i^2\right)^2 - 2\sum_{i=1}^{3} l_i^4\right\}^{\frac{1}{2}} \tag{15}$$

is the area of the triangle formed by the $\hat{\Gamma}_i$'s. As well as giving a measure of uncertainty, $\hat{\sigma}$ can also be used to alert the operator to the use of a calibration which is no longer valid, to the presence of harmonics, or to other inconsistencies invalidating the calibration.

## VI. A Comparison of Some Six-Port Junction Designs

In Section IV, we used the MSD of $(\hat{\mu}, \hat{\nu})$ from $(\mu, \nu)$ as a simple rotationally invariant measure of the adequacy of the linear approximation to our model. Of course, it also gives a measure of how precise $(\hat{\mu}, \hat{\nu})$ is as an estimator of $(\mu, \nu)$, and provided the linear approximation is adequate, (12) gives an approximate value of this measure for any given $\sigma^2$ and any angular configuration of circle centers about $(\mu, \nu)$. In fact, for the purposes of comparing the five six-port junction designs mentioned in the Introduction, we shall compute the standardized root-mean-squared distance, $\mathrm{SRMSD} \equiv (\mathrm{MSD})^{\frac{1}{2}}/\sigma$, which is easily obtained from (12).

Relevant details of the five six-port junction designs mentioned in the Introduction are given in Table I. In the table, the locations of the circle centers are given in polar coordinate form, i.e., $(S_i, \psi_i)$, where $\xi_i = S_i\cos\psi_i$, $\eta_i = S_i\sin\psi_i$, $i = 1,2,3$.

For the five designs and with $\rho = 0$ and $\rho = 0.5$, the SRMSD was computed as the *true* intersection point $\Gamma$ ranged over the area of the Smith chart (passive impedances), i.e., the unit circle. Contour plots of the SRMSD for the five designs when $\rho = 0.5$ are shown in Figs. 2–6. (Remember that $\rho = 0.5$ corresponds approximately to the case where all four power meter readings have the same signal-to-noise ratio.) In the plots, points of constant SRMSD are connected, in SRMSD increments of 0.05. When $\rho = 0.5$, the minimum achievable value of SRMSD is $(2/3)^{\frac{1}{2}} \doteq 0.816$ and this is achieved when $\delta_1 = \delta_2 = \delta_3 = 2\pi/3$. Noting that lower SRMSD values indicate a better performance, it is seen that the idealized six-port represented in Fig. 2 performs best overall. The practical com-

TABLE I
LOCATIONS OF THREE CIRCLE CENTERS IN POLAR COORDINATE FORM

| Reference | $(S_1, \psi_1^o)$ | $(S_2, \psi_2^o)$ | $(S_3, \psi_3^o)$ | Fig. No. |
|---|---|---|---|---|
| Engen [11] | (1.5,0) | (1.5,120) | (1.5, −120) | 2 |
| Engen and Hoer [13] | ($\sqrt{2}$,0) | (2, 135) | (2, −135) | 3 |
| Groll and Kohl [14] | (1,180) | (1, −90) | (0, − ) | 4 |
| Somlo and Hunter [7] | (1.92,0) | (1.92,90) | (1.92, −90) | 5 |
| Griffin et al [15] | (1,0) | (3,109) | (3, −109) | 6 |

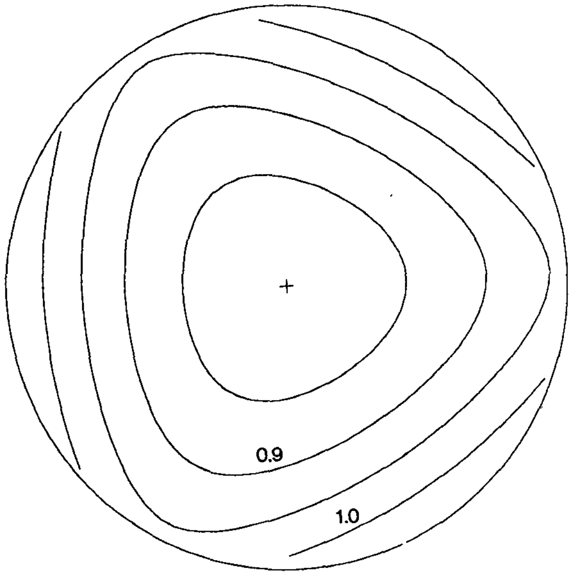


Fig. 2. Contour plot of SRMSD as Γ ranges over the unit circle for the design of Engen [11] when $\rho = 0.5$. See Table I for details.

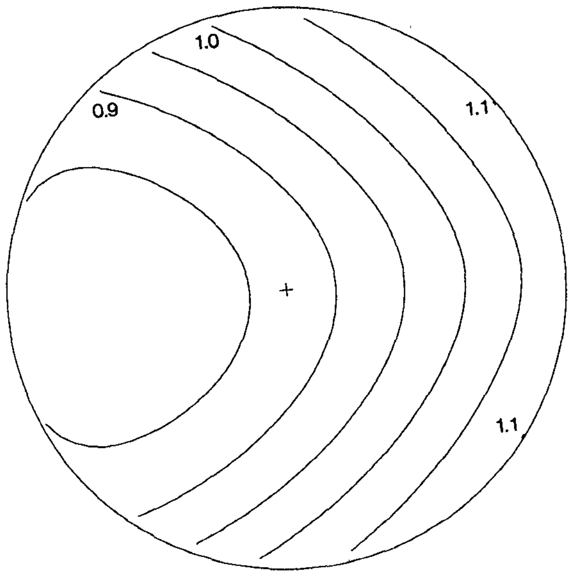


Fig. 3. Contour plot of SRMSD as Γ ranges over the unit circle for the design of Engen and Hoer [13] when $\rho = 0.5$. See Table I for details.

promises represented in Figs. 3 and 5 are only a little poorer. The six-ports of Fig. 6 and especially Fig. 4 are noticeably poorer, especially near the perimeter of the Smith chart. The contours in Fig. 4 near the origin and in

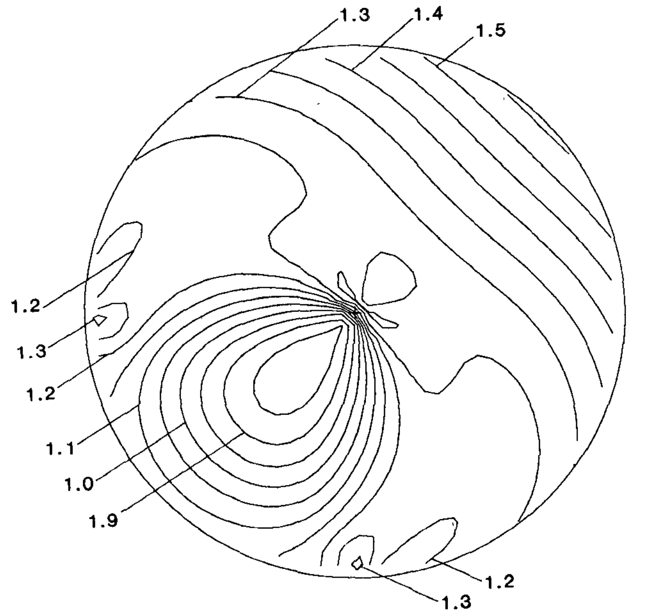


Fig. 4. Contour plot of SRMSD as Γ ranges over the unit circle for the design of Groll and Kohl [14] when $\rho = 0.5$. See Table I for details.

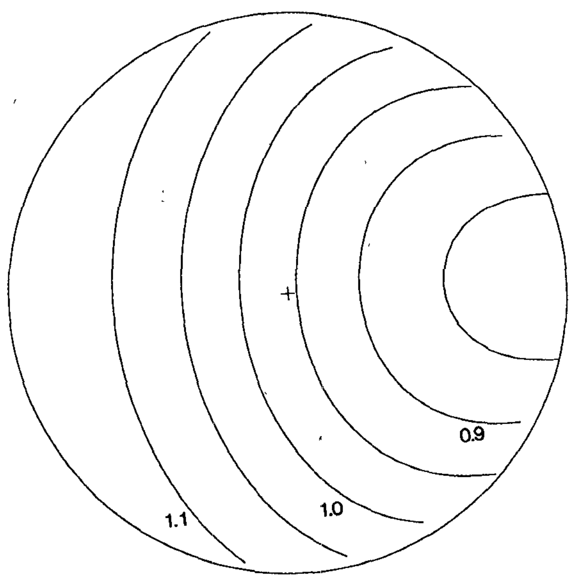


Fig. 5. Contour plot of SRMSD as Γ ranges over the unit circle for the design of Somlo and Hunter [7] when $\rho = 0.5$. See Table I for details.

Fig. 6 near (1,0) should be treated with care, for these points are circle centers for their respective designs. If Γ is near some $C_i$, $R_i$ is small and so the signal-to-noise ratio may be very small here. The linear approximation used to derive (12) is no longer valid in such a region. When $\rho = 0$, the qualitative conclusions are similar to those when $\rho = 0.5$.

## VII. Summary and Discussion

A statistically based method for permitting an objective comparison of different six-port designs has been given. A function which measures the uncertainty due to noise in the approximately optimal estimator of Γ has been plotted over the area of the Smith chart for several designs.

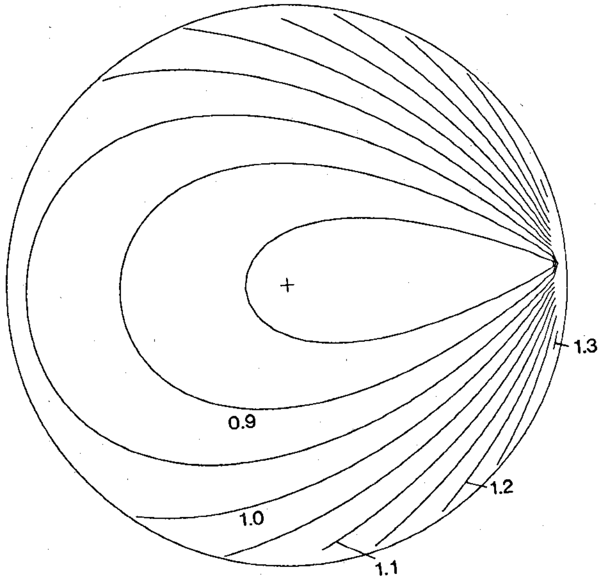


Fig. 6. Contour plot of SRMSD as $\Gamma$ ranges over the unit circle for the design of Griffin *et al.* [15] when $\rho = 0.5$. See Table I for details.

The estimated value of $\Gamma$ suggested in this paper is given by (6). It is optimal in the sense that, when noise is present, it is the linear combination of the three intersection points which is minimum variance unbiased for both its coordinates.

Finally, we notice that the method of estimation given in this paper may have application to navigation systems based on the measurement of distances from three fixed transmitters (e.g., the Omega circular radio navigation system [18]).

## Acknowledgment

The authors wish to thank S. Clancy for helping to produce Figs. 2–6.

## References

[1] G. F. Engen and C. A. Hoer, "Application of arbitrary 6-port junctions to power-measurement problems," *IEEE Trans. Instrum. Meas.*, vol. IM-21, pp. 470–474, Nov. 1972.
[2] C. A. Hoer, "The six-port coupler: A new approach to measuring voltage, current, power, impedance, and phase," *IEEE Trans. Instrum. Meas.*, vol. IM-21, pp. 466–470, Nov. 1972.
[3] M. D. Rafal and W. T. Joines, "Optimizing the design of the six-port junction," in *IEEE MTT-S Int. Microwave Symp. Dig.*, 1980, pp. 437–439.
[4] L. Kaliouby and R. G. Bosisio, "A new method for six-port swept frequency automatic network analysis," *IEEE Trans. Microwave Theory Tech.*, vol. MTT-32, pp. 1678–1682, Dec. 1984.
[5] G. F. Engen, "A least squares solution for use in the six-port measurement technique," *IEEE Trans. Microwave Theory Tech.*, vol. MTT-28, pp. 1473–1477, Dec. 1980.
[6] B. A. Herscher and J. E. Carroll, "Optimal use of redundant information in multiport reflectometers by statistical methods," *Proc. Inst. Elec. Eng.*, pt. H, vol. 131, pp. 25–31, Feb. 1984.
[7] P. I. Somlo and J. D. Hunter, "A six-port reflectometer and its complete characterization by convenient calibration procedures," *IEEE Trans. Microwave Theory Tech.*, vol. MTT-30, pp. 186–192, Feb. 1982.
[8] J. D. Hunter and P. I. Somlo, "An explicit six-port calibration method using five standards," *IEEE Trans. Microwave Theory Tech.*, vol. MTT-33, pp. 69–72, Jan. 1985.
[9] P. I. Somlo, J. D. Hunter, and D. C. Arthur, "Accurate six-port operation with uncalibrated nonlinear diodes," *IEEE Trans. Microwave Theory Tech.*, vol. MTT-33, pp. 281–282, Mar. 1985.
[10] P. I. Somlo, "The locating reflectometer," *IEEE Trans. Microwave Theory Tech.*, vol. MTT-20, pp. 105–112, Feb. 1972.
[11] G. F. Engen, "Design considerations for automatic network analyzers based on the six-port concept," in *Europ. Conf. Prec. Elect. Meas., Euromes-77*, 1977, pp. 110–112.
[12] J. D. Hunter and P. I. Somlo, "Simple derivation of six-port reflectometer equations," *Electron. Lett.*, vol. 21, pp. 370–371, Apr. 1985.
[13] G. F. Engen and C. A. Hoer, "Application of an 'arbitrary' 6-port junction to power measurement problems," *CPEM Dig.*, 1972, pp. 100–101.
[14] H. P. Groll and W. Kohl, "Six port consisting of two directional couplers and two voltage probes for impedance measurement in the millimeter-wave range," *IEEE Trans. Instrum. Meas.*, vol. IM-29, pp. 386–390, Dec. 1980.
[15] E. J. Griffin, G. J. Slack, and L. D. Hill, "Broadband six-port reflectometer junction," *Electron. Lett.*, vol. 19, pp. 921–922, Oct. 1983.
[16] P. I. Somlo and J. D. Hunter, *Microwave Impedance Measurement*. London: Peregrinus, 1985, ch. 7.2.2.
[17] C. R. Rao, *Linear Statistical Inference and its Applications*, 2nd ed. New York: Wiley, 1973, ch. 4a.
[18] *Omega Navigation System User Guide*, International Omega Association, 1978.

**Michael J. Buckley** was born in Sydney, Australia, in 1960. He graduated from the University of Sydney in 1982, receiving the B.Sc. (Hons.) in mathematical statistics.

Since 1984 he has been an Experimental Scientist at the CSIRO Division of Mathematics and Statistics, where he consults with the CSIRO Division of Food Research and the CSIRO Wheat Research Unit. His research interests include spline smoothing and other aspects of nonparametric regression.

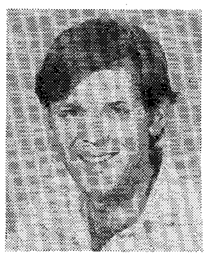

**Mark Berman** was born in Sydney, Australia, in 1951. He received the B.Sc. (Hons.) and University Medal in mathematical statistics from the University of New South Wales in 1974, and the Master of Statistics from the same institution in 1976. In 1978, he was awarded the Ph.D. and D.I.C. in mathematical statistics by the Imperial College of Science and Technology, London.

He was a Visiting Lecturer in the Department of Statistics at the University of California, Berkeley, during 1978–79, and since 1979 he has been with the CSIRO Division of Mathematics and Statistics, Sydney, where he is now a Senior Research Scientist. He regularly consults and collaborates with members of the CSIRO Divisions of Applied Physics, and Mineral Physics and Mineralogy, and his research interests cover a range of topics in both applied and theoretical statistics.

**Peter I. Somlo** (SM'71–F'87) was born in Budapest, Hungary. He graduated (Dipl. Ing.) from the University of Technology of Budapest in 1956.

In 1957 he joined the National Measurement Laboratory (then National Standards Laboratory) of the CSIRO, Sydney, Australia, where he is now a Senior Principal Research Scientist and leader of the Rf/Microwave Group. His work involves the coordination of the microwave calibration service, including the design and operation of microwave standards and the associated measuring techniques. Mr. Somlo was an invited lecturer at the University of Sydney for a one-term course on high-frequency measurement methods, and he was an invited keynote speaker at the inaugural Asia-Pacific Microwave Conference.

Mr. Somlo is the author of over 50 publications, including an invited paper for the PROCEEDINGS OF THE IEEE. He is senior coauthor of the book *Microwave Impedance Measurements* and is the joint inventor of three patents. He has been a member of the Editorial Review Board of the *IEEE Transactions on Microwave Theory and Techniques* since 1970 and is a former Vice Chairman of the IEEE Australian Section. Mr. Somlo is the Australian Representative of Commission A of URSI (International Union of Radio Science), and in 1984 he was awarded the IEEE Centennial Medal.